Development of molecular and cellular tools to decipher the type I IFN pathway of the common vampire bat

Sarkis Sarkis, Marie-Claude Lise, Edith Darcissac, Stéphanie Dabo, Marcel
Falk, Laura Chaulet, Christine Neuveut, Eliane Meurs, Anne Lavergne,
Vincent Lacoste

Development of molecular and cellular tools to decipher the type I IFN pathway of the common vampire bat

Sarkis Sarkis [a, *], Marie-Claude Lise [a], Edith Darcissac [a], Stéphanie Dabo [b], Marcel Falk [a], Laura Chaulet [a], Christine Neuveut [b], Eliane F. Meurs [b], Anne Lavergne [a], Vincent Lacoste [a, **]

[a] Laboratoire des Interactions Virus-Hôtes, Institut Pasteur de La Guyane, Cayenne, French Guiana
[b] Hepacivirus and Innate Immunity, Institut Pasteur, 75015 Paris, France

ABSTRACT

Though the common vampire bat, *Desmodus rotundus*, is known as the main rabies virus reservoir in Latin America, no tools are available to investigate its antiviral innate immune system. To characterize the IFN-I pathway, we established an immortalized cell line from a *D. rotundus* fetal lung named FLuDero. Then we molecularly characterized some of the Toll-like receptors (TLR3, 7, 8 and 9), the three RIG-I-like receptor members, as well as IFNα1 and IFNβ. Challenging the FLuDero cell line with poly (I:C) resulted in an up-regulation of both IFNα1 and IFNβ and the induction of expression of the different pattern recognition receptors characterized. These findings provide evidence of the intact dsRNA recognition machinery and the IFN-I signaling pathway in our cellular model. Herein, we generated a sum of insightful specific molecular and cellular tools that will serve as a useful model to study virus–host interactions of the common vampire bat.

1. Introduction

After Rodentia, the Chiroptera order is the most diverse and geographically widespread mammalian order, accounting for one-fifth of all classified living mammals (Simmons, 2005). Bats are also known to harbor emerging and re-emerging zoonotic viruses, many of which cause severe morbidity and mortality in humans and other mammals (Moratelli and Calisher, 2015). Most of these viruses seem to be harmless or only rarely associated with clinical signs in bats under natural or experimental infection (Middleton et al., 2007; Paweska et al., 2015; Sulkin et al., 1966; Watanabe et al., 2010). Strikingly, mechanisms that allow bats to coexist with these highly lethal viruses remain poorly understood (Baker et al., 2013). Different hypotheses have been emitted. One of these assumptions is based on the capacity of their innate immune system to rapidly control viral replication after infection. In mammals, innate immune recognition depends on the detection of constitutive and conserved patterns in microbes, the pathogen-associated molecular patterns (PAMPs), by a variety of pattern recognition receptors (PRRs) (Takeda et al., 2003). Among the four distinct groups of PRRs identified to date (Thompson et al., 2011), the Toll-like receptors (TLRs) are expressed in immune as well as non-immune cells (Akira, 2006) and can be distinguished according to their cell location. While some TLRs (TLR1, 2, 4, 5, 6 and 10) are expressed on the cell surface, TLR 3, 7, 8 and 9 are almost exclusively located intracellularly at the endosomes (Xiao, 2009). In addition, whereas surface-expressed TLRs are mainly involved in the recognition of bacterial and fungal cell wall components as well as of some viral proteins, the intracellular/endosomal TLRs detect microbial nucleic acids (Xiao, 2009).

Apart from endosomal sensing by TLRs, viral RNA can also be detected by a second class of PRRs, the retinoic acid-inducible gene (RIG)-I-like receptors (RLRs), expressed in the cytosol of a ubiquitous type of cells (Yoneyama et al., 2004). Three RLR members have been identified to date: RIG-I, melanoma differentiation antigen 5 (MDA5) and laboratory of genetics and physiology 2 (LGP2) (Yoneyama and Fujita, 2010). They belong to the DExD/H box family

* Corresponding author. Laboratoire des Interactions Virus-Hôtes, Institut Pasteur de la Guyane, 23 avenue Pasteur, 97300 Cayenne, French Guiana.
** Corresponding author. Laboratoire des Interactions Virus-Hôtes, Institut Pasteur de la Guyane, 23 avenue Pasteur, 97300 Cayenne, French Guiana.
E-mail addresses: ssarkis@pasteur-cayenne.fr (S. Sarkis), vlacoste@pasteur-cayenne.fr (V. Lacoste).

of helicases, known for their important cellular functions in promoting RNA conformational changes and annealing RNA strands, and for their ability to unwind double-stranded RNA. Contrary to MDA5 and RIG-I, the role of LGP2 in innate immunity remains unclear. While some studies propose that LGP2 functions by modifying viral RNA to facilitate its recognition by RIG-I or MDA5 (Moresco and Beutler, 2010), others describe LGP2 as a positive and negative regulator of MDA5-and RIG-I-dependent responses, respectively (Takahasi et al., 2009).

PAMPs' recognition by the PRRs results in the release of type I IFNs (IFN-I) (different subtypes of IFNα and one IFNβ) and type III IFNs (IFNλ1 and IFNλ2/3) as well as of chemokines and proinflammatory cytokines. This leads to an "antiviral state" and orients the adaptive immune response (Loo and Gale, 2011). Then, upon binding to their cognate receptors, IFN triggers the production of hundreds of IFN-stimulated genes (ISGs), which are associated with its antiviral activity.

Only a few studies are available on the immune system of bats, essentially restricted to Old World species. Most studies have been conducted on the black flying fox (*Pteropus alecto*). Similarly to humans, sheep, cows and pigs, *P. alecto* transcribes ten different functional TLR genes (TLR1-10) and a TLR13-like pseudogene. Some of these TLRs, specifically those involved in viral recognition, have been described in other bat species such as *Rousettus leschenaulti* (Iha et al., 2010), the common vampire bat, *Desmodus rotundus*, as well as in other New and Old World species (Escalera-Zamudio et al., 2015; Jiang et al., 2017; Schad and Voigt, 2016; Shaw et al., 2012). The three RLR members, RIG-I, MDA5 and LGP2, have also been described in bats from the *Pteropus* and *Myotis* genera (Cowled et al., 2012; He et al., 2014).

We recently reported circulation of the rabies virus in different bat species in French Guiana, South America, where approximately 100 bat species are present (de Thoisy et al., 2016). We also demonstrated that circulation of the virus was favored in forest areas in which bat species with a hematophagous diet, such as *D. rotundus*, play a major role. Furthermore, this species has been described as being able to cope with rabies virus infection (Aguilar-Setien et al., 2005). We therefore considered that there was a crying need for investigating the innate immune system of *D. rotundus* to understand how they manage viral infections. Our first objective was therefore to molecularly characterize some of the PRRs implicated in viral recognition. We focused our attention on some of the TLRs (TLR3, 7, 8 and 9); RLR, RIG-I, MDA5 and LGP2; as well as on type I IFN (IFNα1 and IFNβ). The second objective was to generate immortalized cell lines of different cell types to provide reproducible data under controlled culture, treatment and infection conditions. Here, we describe the characterization of the targeted genes and the establishment of an immortalized lung cell line obtained from the fetal lung tissue of a *D. rotundus* bat, which we named FLuDero. Development of these tools allowed us to characterize the innate immune competency of the cell line obtained in a time-course study after poly (I:C) transfection. This study offers new insights into deciphering the innate immune defense of the common vampire bat that could be applied to the study of a number of different viral families, first and foremost rabies virus.

2. Materials and methods

2.1. Ethics statement

The animal was captured, handled and sampled following ASM guidelines (Sikes and Gannon, 2011) under the supervision of researchers with a French level 1 animal experimentation degree. Even though bats are not protected by law in French Guiana, the project was submitted to the Conseil Scientifique Régional pour le Patrimoine Naturel de la Guyane and approved under authorization number 59 obtained 04/17/2013 delivered by the Prefecture of French Guiana.

2.2. Animal, tissue collection and cell culture

A *D. rotundus* pregnant female was caught in a breeding cave in French Guiana, using a mist net. The bat was anesthetized with 0.05 mg of Ketamine (Kétamine 1000®) and 0.01 mg of Xylazine (Nerfasin Vet®) and euthanized with an intracardiac injection of pentobarbital sodium (Dolethal®). After euthanasia, brain, liver, kidney, spleen, trachea and fetal lung tissues were collected and roughly washed in sterile phosphate buffered saline (PBS 1X) containing 100 units/ml penicillin and 100 μg/ml streptomycin (Sigma). Then the organs were cleaned of the attached surrounding tissue, chopped into small pieces with a sterile blade and cultured in six-well cell culture plates in prewarmed DMEM/Ham's Nutrient Mixture F12 (Sigma) supplemented with 10% fetal bovine serum (FBS) (Sigma), 100 units/ml penicillin and 100 μg/ml streptomycin. Organ pieces were maintained in a humidified incubator with 5% CO_2 at 37 °C and allowed to settle and attach for one week. The cells were observed daily for quality and outgrowth. The culture medium was removed after 3–5 days and replaced with fresh medium. After expansion of primary cells to confluent monolayer cells, these cells were conserved in liquid nitrogen. Fetal lung primary cells were immortalized by transduction as described previously (Crameri et al., 2009; Hofmann et al., 2006) using lentiviral particles expressing the Simian Virus 40 Early Region, encoding the large T and the small t antigen. This required that 2.6 Kb SV40 TAg be inserted into the lentiviral HR′TRIPΔU3 (Zennou et al., 2000) under the EF1α promoter (C. Neuveut; unpublished data). Two to three weeks following immortalization, when an increase in cell growth was observed, cells were verified for expression of SV40 large T antigen by immunoblot analysis. After the fifth passage, immortalized cells were subcloned by end-point-limiting dilution. Cell populations initially derived from a single cell and presenting the same morphology as the primary cells were selected. Once the cells had grown to 70% confluence, they were passaged into larger flasks to expand them before storage in liquid nitrogen. The obtained cell line has been named FLuDero for Fetal Lung *D. rotundus*.

2.3. Immunoblot analysis

Five millions of cells were washed once with PBS and scraped into CHAPS buffer (50 mM Tris-HCl pH 7.5, 140 mM NaCl, 5 mM EDTA, 5% glycerol, 1% CHAPS) that contained phosphatase and protease inhibitors (Complete, Roche Applied Science). The protein concentration was determined according to Bradford. Protein electrophoresis was performed on NuPAGE 4–12% Bis TRIS gels (Invitrogen). Proteins were transferred onto nitrocellulose membranes (Fisher Bioblock Scientific) and probed with mouse monoclonal anti-SV40 T antigen (sc-55461; Santa Cruz Biotechnology) and anti-β-actin antibody (A1978; Sigma). For secondary antibodies, we used Goat anti-Mouse IgG (H + L) IrDye 700 (Li-Cor). Fluorescent immunoblot images were acquired and quantified by using an Odyssey scanner and the Odyssey 3.1 software (Li-Cor Biosciences).

2.4. RNA extraction and cDNA synthesis

To generate the full-length coding sequences of the targeted genes, total RNA was extracted from either liver tissue or poly (I:C) (Sigma, cat #P9582) transfected lung FLuDero cells (see below) using TRIzol Reagent (Invitrogen) as recommended by the manufacturer. cDNAs were synthesized using Superscript®III reverse

transcriptase (Invitrogen) and random hexamers following the manufacturer's instructions.

2.5. Sequence identification and domain characterization

All amplifications to generate the full-length coding sequences of TLR3, 7, 8 and 9, RIG-I, MDA5, LGP2 as well as IFNα1 and partial β-actin sequence were performed on cDNA obtained from liver-extracted RNA, while the complete sequence of IFNβ was obtained using RNA extracted from the poly (I:C) transfected FLuDero cell line. Internal coding regions were amplified by PCR using the AmpliTaq Gold DNA polymerase kit (Thermo Fischer Scientific). Different combinations of consensus and specific degenerate primers were designed using Primer3 (v.0.4.0) based on alignments of orthologous mammal sequences (bat, equine, swine, feline, bovine and human) available in the GenBank database (Supplementary Table 1). The 5′- and 3′-terminal sequences were obtained by rapid amplification of cDNA ends (RACE) using the FirstChoice® RLM-RACE Kit (Ambion, Inc.). PCR and RACE products were cloned using the pCR™4-TOPO® TA Cloning® Kit (Invitrogen). The sequences obtained were confirmed by similarity analysis using the NCBI BLAST search (http://www.ncbi.nlm.nih.gov/BLAST). Structural domains of RLRs were identified using SMART software (http://smart.embl-heidelberg.de/) (Letunic et al., 2015).

2.6. RLRs phylogenetic analysis

The complete coding sequences for RIG-I, MDA-5, LGP2, IFNα1 and IFNβ of representative Laurasiatherian and Euarchontoglires and of a marsupial (Monodelphis domestica) were downloaded from the NCBI Database. Three (IFNα1), nine (MDA-5, LGP2) and ten (RIG-I, IFNβ) bat sequences were available (Supplementary Table 2). The sequences of D. rotundus obtained in this study were further added to each data set. After alignment and editing, the MEGA version 6.0 software (Tamura et al., 2013) was used to determine the best-fit amino acid evolutionary substitution model (Jones-Taylor-Thornton + G + F), and phylogenetic analyses were performed under maximum-likelihood criteria with 500 bootstrap replicates. All trees were rooted with the marsupial Monodelphis domestica or rodent Mus musculus sequences.

2.7. Poly(I:C) stimulation, RNA extraction and cDNA synthesis

Pulmonary fetal cells were seeded in 12-well plates at a density of 2.5×10^5 cells/well and cultured as described above. Twenty hours after seeding, cells were stimulated by transfection with 20 μg/ml of poly (I:C) by calcium phosphate transfection (Invitrogen). Cells were harvested in TRIzol Reagent at 0, 3, 6, 9, 12, 24, 48 and 72 h post-stimulation and stored at −80 °C until RNA extraction. The cDNA was synthesized as described above (for each sample, 200 ng of total RNA was used as template for cDNA synthesis). The experiment was performed three times.

2.8. Quantitative PCR

Quantitative PCR (qPCR) was performed on a StepOne™ Real-Time PCR System using the TaqMan®Universal PCR Master Mix (Applied Biosystems). Primers and TaqMan® probes were designed using Primer Express 3.0 (Applied Biosystems) (Supplementary Table 1). Each reaction was performed in duplicate. The cycling conditions were those recommended by the manufacturer: 55 °C for 2 min, 95 °C for 2 min followed by 40 cycles at 95 °C for 15 s, 60 °C for 1 min. For absolute quantification, the exact number of copies of the gene of interest was calculated using a plasmid DNA standard curve. Individual expression values were normalized and

compared to mRNA encoding β-actin. Values are shown graphically as fold induction compared to the mock sample (0 h transfection) for each experiment.

3. Results

3.1. Establishment of a clonal fetal D. rotundus cell line

Fetal lung tissue was collected from a pregnant female D. rotundus. During the 1st week of culture, outgrowth of primary cells from chopped tissue was observed. After immortalization through transduction of lentiviral particles expressing the SV40 large T antigen and small t antigen, a broad spectrum of distinct cellular morphologies was observed, ranging from predominant fibroblast-to epithelial-like cells. With each subsequent subculture, the cellular population became more homogeneous given that the faster growing cells predominated. After the fifth passage, end-point dilution plating was performed to prepare clonal cell lines. One cell line, named FLuDero, was maintained in culture. The expression of SV40T antigen in this cell line was verified by western blot analysis (Supplementary Fig. S1).

3.2. D. rotundus PRRs and IFN-I sequence characterization

Full-length coding sequences of the selected TLRs (3, 7, 8 and 9) and RLR members (RIG-I, MDA5 and LGP2) as well as of IFNα1 were obtained from mRNA directly extracted from the liver tissue of the D. rotundus bat, revealing a constitutive expression of these genes. In contrast, the IFNβ coding sequence was only obtained after poly (I:C) stimulation of the established FLuDero cell line. Sequence analysis revealed that the coding regions of D. rotundus cDNA for TLR3, 7, 8 and 9, were 2712, 3150, 3123 and 3096 bp in length, respectively, with open reading frames encoding 903, 1049, 1040 and 1032 amino acids (aa), respectively. These TLR sequences shared more than 99% identity at the nucleotide and protein levels with the previously published Mexican D. rotundus sequences (TLR3: KR349157, TLR7: KR349160, TLR8: KR349163, and TLR9: KR349164) (Escalera-Zamudio et al., 2015). The full-length sequences of D. rotundus RIG-I, MDA5, LGP2, IFNα1 and IFNβ were 2787, 3063, 2025, 567 and 564 bp in length, encoding putative proteins of 928, 1020, 674, 188 and 187 aa, respectively. D. rotundus RLR nucleotide and amino acid sequences shared a high level of similarity with their mammal counterparts (Supplementary Table 3). For instance, MDA5 appeared to be the most highly conserved RLR member, sharing 86−87% amino acid sequence identity with its equine, canine, bovine and human homologs. RIG-I and LGP2 shared slightly less similarity with their mammal counterparts, exhibiting 80−83% amino acid sequence identity. The D. rotundus RIG-I-, MDA5-and LGP2-encoded proteins presented a similar structural domain organization to that seen in their mammalian homologs. Indeed, sequence analysis of RIG-I and MDA5 showed that these two proteins possess two N-terminal tandem caspase activation and recruitment domains (CARDs), followed by a central DEAD box helicase domain, including a DExD/H box helicase domain and a helicase C-terminal domain (HELICc), and a C-terminal domain (CTD) containing the RIG-I regulatory domain (RIG-I-C_RD) (Supplementary Fig. S2). Similarly to the sequence of LGP2 from other mammals, the D. rotundus LGP2 lacks CARD domains at its N terminus and presents a DExD/H box helicase, a helicase-conserved C-terminal domain and a CTD (Supplementary Fig. S2). In comparison, IFNα1 and IFNβ shared limited sequence identities with their mammal counterparts. D. rotundus IFNα1 shared a maximum 73% sequence identity at the protein level with its most related mammal homolog, equine IFNα1. IFNβ showed lower similarity with its mammalian homologs,

ranging from 50 to 60% at the amino acid level. Through phylogenetic analyses, we then showed that all the *D. rotundus* sequences generated belonged to a single clade of chiropters (Supplementary Figs. S3 and S4). The phylogenetic trees generated were in agreement with the different mammalian orders. Nevertheless, for the RLRs, the relationships between these orders were weakly supported by bootstrap analysis (Supplementary Fig. S3). These sequences were submitted to GenBank under accession numbers MF121906−MF121914.

3.3. Distinct expression profile of type I interferon in D. rotundus lung cell line

We next investigated whether the IFN-1 system was functional in the immortalized FLuDero cell line by studying the kinetics of induction of IFNβ and IFNα1, at the RNA level using RTqPCR, following transfection of the cells with poly (I:C) (Fig. 1). The basal expression levels of both RNA were at the limit of detection in the absence of treatment (Fig. 2). IFNβ was found to be highly induced with more than 3000-fold up-regulation. It was detected as early as 3 h post-transfection, reaching a peak at 24 h and then declining (Fig. 1a). Conversely, IFNα1 was not significantly up-regulated during the first 12 h after stimulation. However, its expression was found to be strongly enhanced at 24 h (400-fold up-regulation) and still sustained at high levels at later points of the kinetics (Fig. 1b). Therefore, the FLuDero cell line proved to respond well to dsRNA with an early and transient induction of IFNβ followed by a late but sustained induction of IFNα1. Altogether, these data indicate the presence of a functional and robust IFN induction pathway in cells from the vampire bat *D. rotundus*.

3.4. RLRs but not TLRs are highly up-regulated in poly(I:C)-transfected lung cells

We then determined the kinetics of expression of the different PRRs in the FLuDero cell line using RTqPCR after transfection of these cells with poly (I:C). Induction of TLR3 expression was observed 9 h after poly (I:C) transfection, with a peak at 24 h displaying a 17-fold increase, followed by a decline at 48 h (Fig. 3a). Conversely, TLR7, 8 and 9 displayed a phase-shift expression in comparison to TLR3 expression, gradually increasing at 24 h post-transfection until the end of the kinetics analysis (Fig. 3b, c, 3d). The kinetics of expression of RIG-I, MDA5 and LGP2 mRNA revealed a similar induction profile as that of TLR3, reaching a peak of induction between 12 h and 24 h, followed by a gradual decrease afterward (Fig. 4a, b, 4c). Interestingly, the expression levels of the RNAs for TLR3, TLR9 and the three RLRs were already significant in the cells in the absence of treatment with poly (I:C), with particularly strong expression for TLR3 and the RLRs, while those of TLR7 and TLR8 were at the limit of detection as for the two IFNs (Fig. 2). Altogether, these data show that the kinetics of induction of TLR3 and the three RLRs by poly (I:C) are similar to IFNβ kinetics of induction. In contrast, induction of TLR7, 8 and 9 is similar to IFNα1 induction. Moreover, these data show that despite their already significant levels in the absence of treatment, the expression of TLR3 and the RLRs can be further enhanced in response to poly (I:C), confirming a robust and functional IFN induction pathway in those cells.
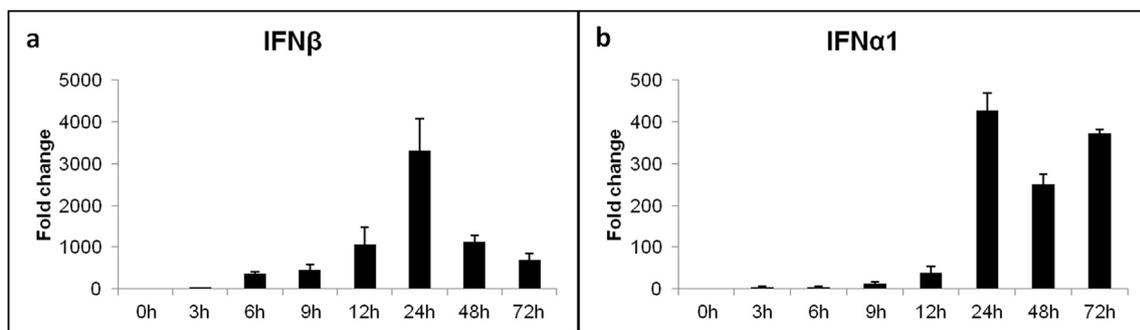

Fig. 1. Poly(I:C) transfection induces expression of IFN-I. Time course fold induction of (**a**) IFNβ and (**b**) IFNα1 in FLuDero cells upon poly (I:C) transfection. IFN-I mRNA were assessed by RTqPCR. Data were normalized against β-actin. Cells were stimulated with 20 μg/ml of poly (I:C) and harvested at the indicated time points. Data represents the mean values of 3 separate experiments, and the error bars represent standard deviations (SD).
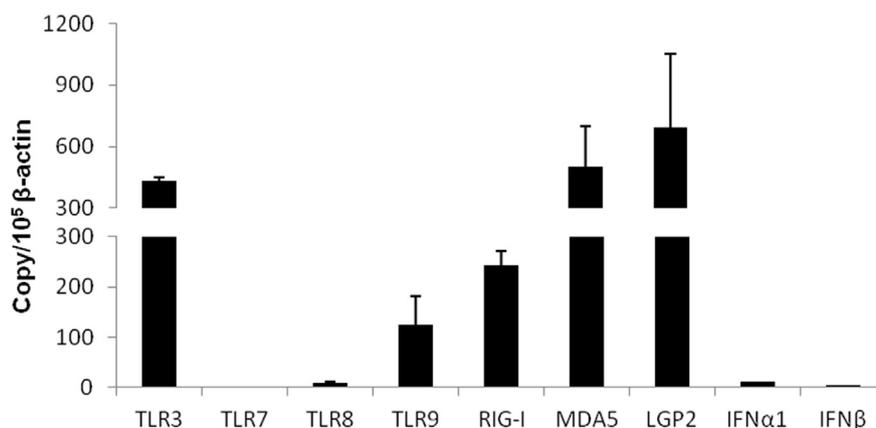

Fig. 2. Basal expression of PRRs and IFN-I in FLuDero. RTqPCR detection of TLR3, 7, 8 and 9, the RLR member, IFNα1 and IFNβ mRNA from unstimulated fetal lung cell from *D. rotundus*. Data were normalized against housekeeping gene β-actin and represents the mean values of 3 separate experiments. The error bars represent standard deviations (SD).
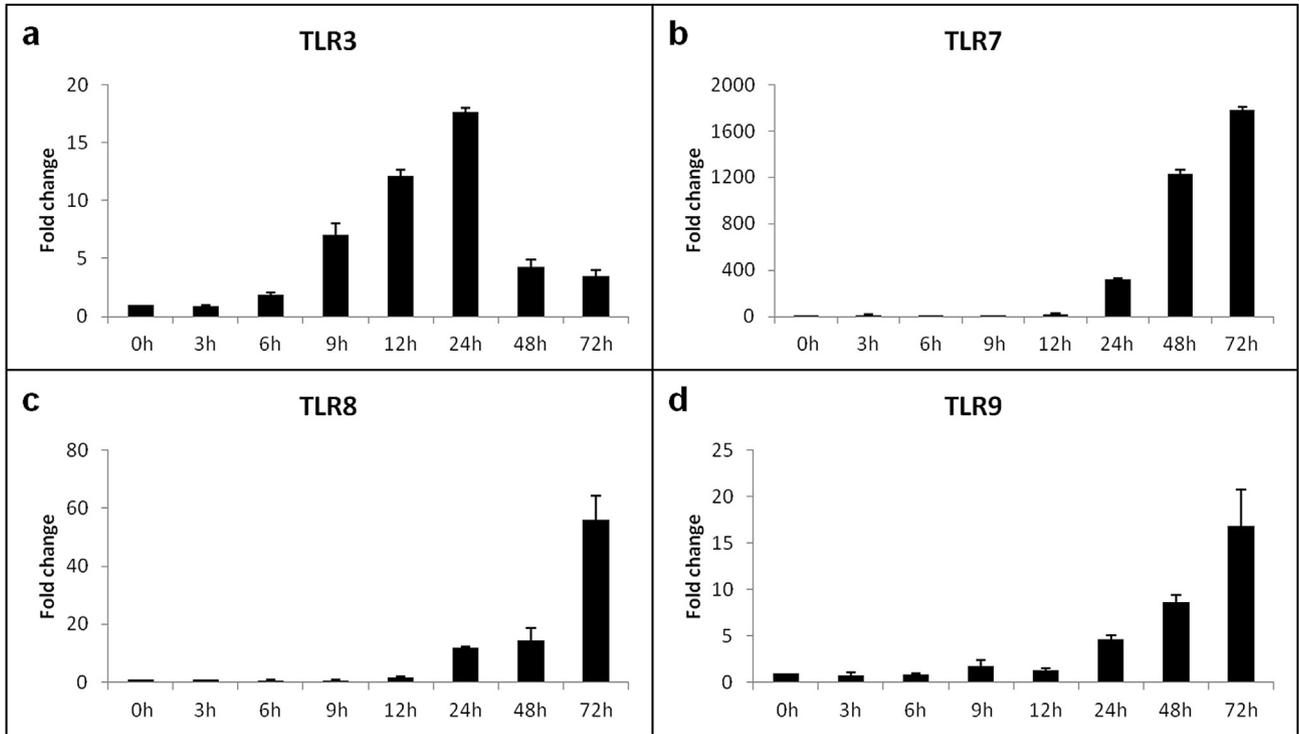
Fig. 3. Poly(I:C) transfection induces expression of endosomal TLRs. Time course fold induction of (**a**) TLR3, (**b**) TLR7, (**c**) TLR8 and (**d**) TLR9 in FLuDero cells upon poly (I:C) transfection. TLRs mRNA were assessed by RTqPCR. Data were normalized against β-actin. Cells were stimulated with 20 μg/ml of poly (I:C) and harvested at the indicated time points. Data represents the mean values of 3 separate experiments, and the error bars represent standard deviations (SD).

Fig. 4. Poly(I:C) transfection induces expression of RLRs. Time course fold induction of (**a**) RIG-I, (**b**) MDA5 and (**c**) LGP2 in FLuDero cells upon poly (I:C) transfection. RLRs mRNA were assessed by RTqPCR. Data were normalized against β-actin. Cells were stimulated with 20 μg/ml of poly (I:C) and harvested at the indicated time points. Data represents the mean values of 3 separate experiments, and the error bars represent standard deviations (SD).
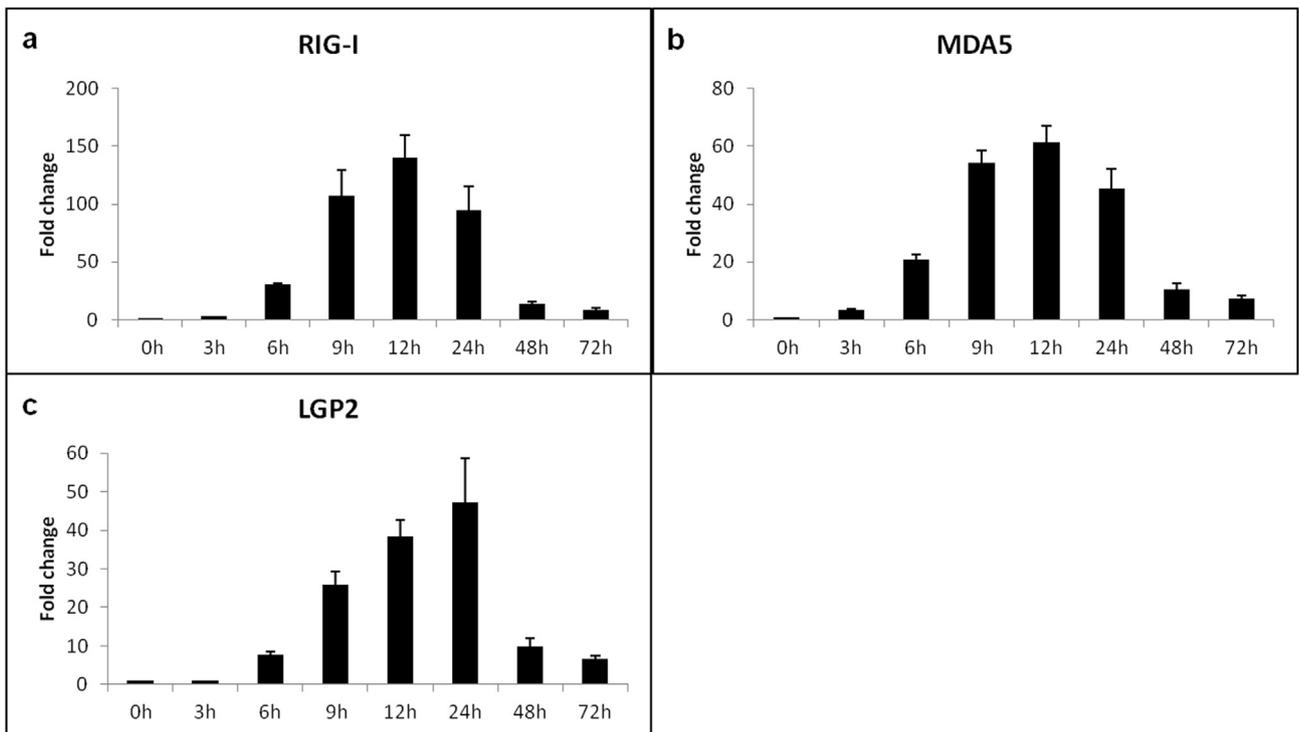
4. Discussion

Emerging infectious diseases caused by bat-borne viruses pose a significant threat to human and animal welfare. With the exception of lyssaviruses (such as rabies), bats harbor highly pathogenic viruses with no clinical signs of disease. One of the possible hypotheses of their asymptomatic status is based on the rapid control of infection by their immune system. To reliably study virus–host interactions, it is important to work on the most pertinent biological models. In this regard, over the last decade, new cell lines have been generated from different bat species (Biesold et al., 2011; Crameri et al., 2009; Eckerle et al., 2014; Hagmaier et al., 2006, 2007; He et al., 2014; Mourya et al., 2013). However, information was still lacking for the common vampire bat, *D. rotundus*, known as a main reservoir for rabies virus, which results in tens of thousands of human deaths every year according to the World Health Organization (2017).

Here, we report the development of a new cell line, FLuDero, generated from fetal lung tissue of a *D. rotundus* bat. In parallel, we molecularly characterized the complete coding sequences of several PRRs involved in viral recognition: TLR3, 7, 8, 9, RIG-I, MDA5 and LGP2, as well as IFNα1 and IFNβ. Our results shows that the TLR3, 7, 8 and 9 share 99% identity at the nucleotide and protein levels with the previously published Mexican *D. rotundus* sequences (Escalera-Zamudio et al., 2015). As previously shown, these TLRs exhibit the genetic characteristics of other mammalian TLRs including a signal peptide, an ectodomain (ligand-binding sites), a highly conserved transmembrane and a TIR domain. Moreover, by characterizing the *D. rotundus* RIG-I, MDA5 and LGP2, we demonstrated that their putative encoded proteins share high structural domain organization with their mammalian counterparts and, as expected, a similar function. High basal levels of TLR3 and RLR mRNAs were observed in FluDero cells, conferring them the capacity to rapidly sense endosomal or cytosolic dsRNAs. Furthermore, the time-course study done after stimulation by poly (I:C) transfection showed two waves of gene induction with an early up-regulation of IFNβ, TLR3, RIG-I, MDA5 and LGP2, followed by a second wave of induction corresponding to the IFNα1, TLR7, 8 and 9.

In host cells, viral recognition is accomplished through two major PRRs, the TLRs and RLRs. Viral or synthetic dsRNA such as poly (I:C) can be sensed by either TLR3 or RLR members depending not only on the structure of RNAs, but also on their entry route. While extracellular dsRNA is thought to activate transcription through endosomal TLR3 following endocytosis, intracellular dsRNA generated during viral replication requires recognition by RLR members such as RIG-I and MDA5 (Akira, 2006; Randall and Goodbourn, 2008; Takeda and Akira, 2005). In our bat cell line, IFNβ was up-regulated early after poly (I:C) transfection, which would more likely result in cytosolic dsRNA recognition by RIG-I and MDA5 considering its entry route, which predominantly reaches the cytosol (Bowie and Unterholzner, 2008; Génin et al., 2009; Honda et al., 2005). In mammals, newly synthesized IFN-I molecules subsequently secreted bind to their cognate receptors and initiate signaling through the JAK/STAT pathway. This cascade leads to a remarkable antiviral state of the infected and neighboring cells and limits the spread of infectious agents. The IFN response mediates its antiviral effects by up-regulating the transcription of hundreds of ISGs, resulting in a significant increase in production of various antiviral effector proteins (Der et al., 1998). Besides their important role as mediators of IFN production, it has also been reported that PRRs' transcription is induced by IFN-α/β, conferring to these genes the status of ISGs (Cowled et al., 2012; Doyle et al., 2003; Heinz et al., 2003; Honda and Taniguchi, 2006; Miettinen et al., 2001; Schneider et al., 2014; Zhou et al., 2011). Our data, demonstrating a concomitant induction of some of these PRRs with

IFNβ, in accord with previous reports, suggest that the positive feedback loop triggering induction of these dsRNA-recognition patterns is essential to enhance the cells' ability to sense dsRNA molecules. Furthermore, this time-course study shows a delayed up-regulation of IFNα1 mRNA observed at the end of the kinetics. It is known that IRF7 is a master positive regulator of IFN-I expression, specifically IFNα. Hence, in a previous study on *P. alecto*, Zhou and colleagues characterized IRF7 as an ISG depending on IFN-I activation (Zhou et al., 2014). Taken together, these data suggest that newly synthesized IRF7 subsequently leads to the induction of large amounts of IFNα genes (Démoulins et al., 2009; Levy, 2002; Marié et al., 1998; van Pesch et al., 2004; Sato et al., 2000). In turn, synthesized IFNα1 may trigger the up-regulation of TLR 7, 8 and 9 in a positive feedback loop, as described in other mammalian species (Guo et al., 2005; Sirén et al., 2005). The present results suggest that, as in other mammalian species, the rapid induction of the IFNβ gene provides an immediate response to virus infection, while the sequential induction of the IFNα1 gene contributes to greatly amplifying the protective response of the cells to viruses (Loo and Gale, 2011; Marié et al., 1998).

Even though our results on PRR expression are congruent with those previously published on *P. alecto*, we obtained delayed kinetics regarding IFN-I expression (Zhou et al., 2011). Nevertheless, the lack of robust cellular identification approaches in bats constitutes a major technical issue and represents a barrier for data comparison. Indeed, species-dependent or cell-dependent factors can explain the differences observed. In addition, these differences can be attributed to the quantity of poly (I:C) used. Indeed, in a previous report, Cowled and colleagues showed in the PaluT02 lung cell line that a large accumulation of poly (I:C) triggers rapid induction of IFN-I in a dose-dependent manner that subsequently leads to the induction of RLR transcription (Cowled et al., 2012).

In conclusion, we have generated a sum of insightful cellular and molecular tools from the common vampire bat species, *D. rotundus*. We found that our clonal immortalized fetal lung cell line is responsive to poly (I:C), a synthetic analog of dsRNA, and that it will therefore be a useful model to study virus–host interactions and antiviral mechanisms. Thus, the mechanisms of cytoplasmic pathogen recognition, the role and contribution of the PRRs, and the IFNs in *D. rotundus*' innate immune response can now be investigated under standardized conditions. These tools will help us in deciphering the cellular and molecular mechanisms implicated in response to viral infection such as rabies virus.

Conflicts of interest

The authors declare that they have no competing interests.

Acknowledgments

Appendix A. Supplementary data

Supplementary data related to this article can be found at

https://doi.org/10.1016/j.dci.2017.10.023.

References

World Health Organization, 2017. Human rabies: 2016 updates and call for data. Releve Epidemiol. Hebd. 92, 77–86.

Aguilar-Setien, A., Loza-Rubio, E., Salas-Rojas, M., Brisseau, N., Cliquet, F., Pastoret, P.P., Rojas-Dotor, S., Tesoro, E., Kretschmer, R., 2005. Salivary excretion of rabies virus by healthy vampire bats. Epidemiol. Infect. 133, 517–522.

Akira, S., 2006. TLR signaling. Curr. Top. Microbiol. Immunol. 311, 1–16.

Baker, M.L., Schountz, T., Wang, L.-F., 2013. Antiviral immune responses of bats: a review. Zoonoses Public Health 60, 104–116.

Biesold, S.E., Ritz, D., Gloza-Rausch, F., Wollny, R., Drexler, J.F., Corman, V.M., Kalko, E.K.V., Oppong, S., Drosten, C., Müller, M.A., 2011. Type I interferon reaction to viral infection in interferon-competent, immortalized cell lines from the African fruit bat Eidolon helvum. PloS One 6, e28131.

Bowie, A.G., Unterholzner, L., 2008. Viral evasion and subversion of pattern-recognition receptor signalling. Nat. Rev. Immunol. 8, 911–922.

Cowled, C., Baker, M.L., Zhou, P., Tachedjian, M., Wang, L.-F., 2012. Molecular characterisation of RIG-I-like helicases in the black flying fox, Pteropus alecto. Dev. Comp. Immunol. 36, 657–664.

Crameri, G., Todd, S., Grimley, S., McEachern, J.A., Marsh, G.A., Smith, C., Tachedjian, M., De Jong, C., Virtue, E.R., Yu, M., et al., 2009. Establishment, immortalisation and characterisation of pteropid bat cell lines. PloS One 4, e8266.

de Thoisy, B., Bourhy, H., Delaval, M., Pontier, D., Dacheux, L., Darcissac, E., Donato, D., Guidez, A., Larrous, F., Lavenir, R., et al., 2016. Bioecological drivers of rabies virus circulation in a neotropical bat community. PLoS Negl. Trop. Dis. 10, e0004378.

Démoulins, T., Baron, M.-L., Kettaf, N., Abdallah, A., Sharif-Askari, E., Sékaly, R.-P., 2009. Poly (I: C) induced immune response in lymphoid tissues involves three sequential waves of type I IFN expression. Virology 386, 225–236.

Der, S.D., Zhou, A., Williams, B.R., Silverman, R.H., 1998. Identification of genes differentially regulated by interferon alpha, beta, or gamma using oligonucleotide arrays. Proc. Natl. Acad. Sci. U. S. A. 95, 15623–15628.

Doyle, S.E., O'Connell, R., Vaidya, S.A., Chow, E.K., Yee, K., Cheng, G., 2003. Toll-like receptor 3 mediates a more potent antiviral response than Toll-like receptor 4. J. Immunol. Balt. Md 1950 170, 3565–3571.

Eckerle, I., Ehlen, L., Kallies, R., Wollny, R., Corman, V.M., Cottontail, V.M., Tschapka, M., Oppong, S., Drosten, C., Müller, M.A., 2014. Bat airway epithelial cells: a novel tool for the study of zoonotic viruses. PloS One 9, e84679.

Escalera-Zamudio, M., Zepeda-Mendoza, M.L., Loza-Rubio, E., Rojas-Anaya, E., Méndez-Ojeda, M.L., Arias, C.F., Greenwood, A.D., 2015. The evolution of bat nucleic acid-sensing Toll-like receptors. Mol. Ecol. 24, 5899–5909.

Génin, P., Vaccaro, A., Civas, A., 2009. The role of differential expression of human interferon–α genes in antiviral immunity. Cytokine Growth Factor Rev. 20, 283–295.

Guo, Z., Garg, S., Hill, K.M., Jayashankar, L., Mooney, M.R., Hoelscher, M., Katz, J.M., Boss, J.M., Sambhara, S., 2005. A distal regulatory region is required for constitutive and IFN-beta-induced expression of murine TLR9 gene. J. Immunol. Balt. Md 1950 175, 7407–7418.

Hagmaier, K., Stock, N., Goodbourn, S., Wang, L.-F., Randall, R., 2006. A single amino acid substitution in the V protein of Nipah virus alters its ability to block interferon signalling in cells from different species. J. Gen. Virol. 87, 3649–3653.

Hagmaier, K., Stock, N., Precious, B., Childs, K., Wang, L.-F., Goodbourn, S., Randall, R.E., 2007. Mapuera virus, a rubulavirus that inhibits interferon signalling in a wide variety of mammalian cells without degrading STATs. J. Gen. Virol. 88, 956–966.

He, X., Korytář, T., Zhu, Y., Pikula, J., Bandouchova, H., Zukal, J., Köllner, B., 2014. Establishment of Myotis myotis cell lines—model for investigation of host-pathogen interaction in a natural host for emerging viruses. PloS One 9, e109795.

Heinz, S., Haehnel, V., Karaghiosoff, M., Schwarzfischer, L., Müller, M., Krause, S.W., Rehli, M., 2003. Species-specific regulation of Toll-like receptor 3 genes in men and mice. J. Biol. Chem. 278, 21502–21509.

Hofmann, A., Kessler, B., Ewerling, S., Kabermann, A., Brem, G., Wolf, E., Pfeifer, A., 2006. Epigenetic regulation of lentiviral transgene vectors in a large animal model. Mol. Ther. J. Am. Soc. Gene Ther. 13, 59–66.

Honda, K., Taniguchi, T., 2006. IRFs: master regulators of signalling by Toll-like receptors and cytosolic pattern-recognition receptors. Nat. Rev. Immunol. 6, 644–658.

Honda, K., Yanai, H., Negishi, H., Asagiri, M., Sato, M., Mizutani, T., Shimada, N., Ohba, Y., Takaoka, A., Yoshida, N., et al., 2005. IRF-7 is the master regulator of type-I interferon-dependent immune responses. Nature 434, 772–777.

Iha, K., Omatsu, T., Watanabe, S., Ueda, N., Taniguchi, S., Fujii, H., Ishii, Y., Kyuwa, S., Akashi, H., Yoshikawa, Y., 2010. Molecular cloning and expression analysis of bat toll-like receptors 3, 7 and 9. J. Vet. Med. Sci. 72, 217–220.

Jiang, H., Li, J., Li, L., Zhang, X., Yuan, L., Chen, J., 2017. Selective evolution of Toll-like receptors 3, 7, 8, and 9 in bats. Immunogenetics 69, 271–285.

Letunic, I., Doerks, T., Bork, P., 2015. SMART: recent updates, new developments and status in 2015. Nucleic Acids Res. 43, D257–D260.

Levy, D.E., 2002. Whence Interferon? Variety in the production of interferon in response to viral infection. J. Exp. Med. 195, f15–f18.

Loo, Y.-M., Gale, M., 2011. Immune signaling by RIG-I-like receptors. Immunity 34, 680–692.

Marié, I., Durbin, J.E., Levy, D.E., 1998. Differential viral induction of distinct interferon-alpha genes by positive feedback through interferon regulatory factor-7. EMBO J. 17, 6660–6669.

Middleton, D.J., Morrissy, C.J., van der Heide, B.M., Russell, G.M., Braun, M.A., Westbury, H.A., Halpin, K., Daniels, P.W., 2007. Experimental Nipah virus infection in pteropid bats (Pteropus poliocephalus). J. Comp. Pathol. 136, 266–272.

Miettinen, M., Sareneva, T., Julkunen, I., Matikainen, S., 2001. IFNs activate toll-like receptor gene expression in viral infections. Genes Immun. 2, 349–355.

Moratelli, R., Calisher, C.H., 2015. Bats and zoonotic viruses: can we confidently link bats with emerging deadly viruses? Mem. Inst. Oswaldo Cruz 110, 1–22.

Moresco, E.M.Y., Beutler, B., 2010. LGP2: positive about viral sensing. Proc. Natl. Acad. Sci. U. S. A. 107, 1261–1262.

Mourya, D.T., Lakra, R.J., Yadav, P.D., Tyagi, P., Raut, C.G., Shete, A.M., Singh, D.K., 2013. Establishment of cell line from embryonic tissue of Pipistrellus ceylonicus bat species from India & its susceptibility to different viruses. Indian J. Med. Res. 138, 224–231.

Paweska, J.T., Jansen van Vuren, P., Fenton, K.A., Graves, K., Grobbelaar, A.A., Moolla, N., Leman, P., Weyer, J., Storm, N., McCulloch, S.D., et al., 2015. Lack of marburg virus transmission from experimentally infected to susceptible in-contact egyptian fruit bats. J. Infect. Dis. 212 (Suppl. 2), S109–S118.

Randall, R.E., Goodbourn, S., 2008. Interferons and viruses: an interplay between induction, signalling, antiviral responses and virus countermeasures. J. Gen. Virol. 89, 1–47.

Sato, M., Suemori, H., Hata, N., Asagiri, M., Ogasawara, K., Nakao, K., Nakaya, T., Katsuki, M., Noguchi, S., Tanaka, N., et al., 2000. Distinct and essential roles of transcription factors IRF-3 and IRF-7 in response to viruses for IFN-alpha/beta gene induction. Immunity 13, 539–548.

Schad, J., Voigt, C.C., 2016. Adaptive evolution of virus-sensing toll-like receptor 8 in bats. Immunogenetics 68, 783–795.

Schneider, W.M., Chevillotte, M.D., Rice, C.M., 2014. Interferon-stimulated genes: a complex web of host defenses. Annu. Rev. Immunol. 32, 513–545.

Shaw, T.I., Srivastava, A., Chou, W.-C., Liu, L., Hawkinson, A., Glenn, T.C., Adams, R., Schountz, T., 2012. Transcriptome sequencing and annotation for the Jamaican fruit bat (Artibeus jamaicensis). PloS One 7, e48472.

Sikes, R.S., Gannon, W.L., 2011. Guidelines of the American Society of Mammalogists for the use of wild mammals in research. J. Mammal. 92, 235–253.

Simmons, N.B., 2005. An eocene big bang for bats. Science 307, 527–528.

Sirén, J., Pirhonen, J., Julkunen, I., Matikainen, S., 2005. IFN-alpha regulates TLR-dependent gene expression of IFN-alpha, IFN-beta, IL-28, and IL-29. J. Immunol. Balt. Md 1950 (174), 1932–1937.

Sulkin, S.E., Allen, R., Sims, R., 1966. Studies of arthropod-borne virus infections in Chiroptera. 3. Influence of environmental temperature on experimental infection with Japanese B and St. Louis encephalitis viruses. Am. J. Trop. Med. Hyg. 15, 406–417.

Takahasi, K., Kumeta, H., Tsuduki, N., Narita, R., Shigemoto, T., Hirai, R., Yoneyama, M., Horiuchi, M., Ogura, K., Fujita, T., et al., 2009. Solution structures of cytosolic RNA sensor MDA5 and LGP2 C-terminal domains: identification of the RNA recognition loop in RIG-I-like receptors. J. Biol. Chem. 284, 17465–17474.

Takeda, K., Akira, S., 2005. Toll-like receptors in innate immunity. Int. Immunol. 17, 1–14.

Takeda, K., Kaisho, T., Akira, S., 2003. Toll-like receptors. Annu. Rev. Immunol. 21, 335–376.

Tamura, K., Stecher, G., Peterson, D., Filipski, A., Kumar, S., 2013. MEGA6: molecular evolutionary genetics analysis version 6.0. Mol. Biol. Evol. 30, 2725–2729.

Thompson, M.R., Kaminski, J.J., Kurt-Jones, E.A., Fitzgerald, K.A., 2011. Pattern recognition receptors and the innate immune response to viral infection. Viruses 3, 920–940.

van Pesch, V., Lanaya, H., Renauld, J.-C., Michiels, T., 2004. Characterization of the murine alpha interferon gene family. J. Virol. 78, 8219–8228.

Watanabe, S., Masangkay, J.S., Nagata, N., Morikawa, S., Mizutani, T., Fukushi, S., Alviola, P., Omatsu, T., Ueda, N., Iha, K., et al., 2010. Bat coronaviruses and experimental infection of bats, the Philippines. Emerg. Infect. Dis. 16, 1217–1223.

Xiao, T., 2009. Innate immune recognition of nucleic acids. Immunol. Res. 43, 98–108.

Yoneyama, M., Fujita, T., 2010. Recognition of viral nucleic acids in innate immunity. Rev. Med. Virol. 20, 4–22.

Yoneyama, M., Kikuchi, M., Natsukawa, T., Shinobu, N., Imaizumi, T., Miyagishi, M., Taira, K., Akira, S., Fujita, T., 2004. The RNA helicase RIG-I has an essential function in double-stranded RNA-induced innate antiviral responses. Nat. Immunol. 5, 730–737.

Zennou, V., Petit, C., Guetard, D., Nerhbass, U., Montagnier, L., Charneau, P., 2000. HIV-1 genome nuclear import is mediated by a central DNA flap. Cell 101, 173–185.

Zhou, P., Cowled, C., Todd, S., Crameri, G., Virtue, E.R., Marsh, G.A., Klein, R., Shi, Z., Wang, L.-F., Baker, M.L., 2011. Type III IFNs in pteropid bats: differential expression patterns provide evidence for distinct roles in antiviral immunity. J. Immunol. Balt. Md 1950 186, 3138–3147.

Zhou, P., Cowled, C., Mansell, A., Monaghan, P., Green, D., Wu, L., Shi, Z., Wang, L.-F., Baker, M.L., 2014. IRF7 in the Australian black flying fox, Pteropus alecto: evidence for a unique expression pattern and functional conservation. PloS One 9, e103875.